STRUCTURAL AND PHASE COMPOSITION MODIFICATION OF NANOCRYSTALLINE $Nd_{14}Fe_{79}B_7$ ALLOY DURING THERMOMAGNETIC MEASUREMENTS

N. Talijan[#]*, V. Ćosović*, T. Žák**, A. Grujić*, J. Stajić-Trošić*

*Institute of Chemistry, Technology and Metallurgy,
Njegoševa 12, 11000 Belgrade, Serbia
**Institute of Physics of Materials, AS CR,
Žižkova 22, CZ – 616 62 Brno, Czech Republic

Abstract

Changes in the microstructure parameters, phase composition and magnetic properties of rapid quenched Nd-rich $Nd_{14}Fe_{79}B_7$ alloy caused by thermomagnetic measurement (TM) were studied using XRD methods of phase analysis, crystallite size and lattice microstrain determination. The observed changes were analyzed between the optimized magnetic state of this alloy and state after TM up to 800^oC.

Measurement of magnetic properties was carried out on the SQUID magnetometer at ambient temperature. The obtained experimental results show that the investigated alloy in the optimized magnetic state has nearly monophase composition with predominant content of hard magnetic $Nd_2Fe_{14}B$ phase (up to 95 mass %) with mean crystallite size below 60 nm.

In the state after TM, it was found that the decreased amount of $Nd_2Fe_{14}B$ phase (75 mass%), increased amount of soft magnetic phases, predominantly of Fe_7Nd_5, formation of Nd-rich oxide Nd_2O_3 phase, as well as grain growth have caused the observed quality loss of hard magnetic properties.

Key words: Neodymium rich Nd-Fe-B alloy; Thermomagnetic mesurement; X-ray diffraction; Magnetic properties

---

1. Introduction

The $Nd_2Fe_{14}B$ hard magnetic materials based on rare earth-transition compounds represent the group of the most up to date permanent magnets. Due to their high coercivity and large energy product they are included within a variety of different applications in numerous technical areas. Consequently, the studies of Nd-Fe-B hard magnetic materials have become very significant over the last few decades [1].

The rapid quenched Nd-Fe-B alloys with overstoichiometric Nd content (Nd-rich alloys) in the optimized magnetic state have almost monophase composition and consist predominantly of main hard magnetic $Nd_2Fe_{14}B$ phase. The minor quantities of soft magnetic Nd-rich phases are mainly situated on grain boundaries of $Nd_2Fe_{14}B$ grains, which are essentially magnetically isolated by this intergranular layer of Nd-rich phases. Accordingly, the magnetic properties of Nd rich Nd-Fe-B alloys are under dominant influence of magnetically decoupled grains of the main hard magnetic phase.

This paper covers part of studies of structural and phase composition changes and their influence on magnetic properties of $Nd_{14}Fe_{79}B_7$ alloy in optimized magnetic state and after thermal decomposition induced by thermomagnetic measurement.

2. Experimental

The investigated $Nd_{14}Fe_{79}B_7$ alloy was produced by centrifugal atomization technique. The composition of the parental material was Nd - 32 mass %, Pr - 0.5 mass %, B - 1.2 mass %, Al - 0.3 mass %, Fe - balance. The as quenched powder was annealed at 630°C for 3 minutes. The applied heat treatment regime was optimized in previous investigations [2,3]. Its basic magnetic characteristics in the optimized magnetic state were $_iH_C$ = 16.2 kOe, Br = 7.4 kG and $(BH)_{max}$ = 10.6 MGOe.

TM analysis was performed in the temperature interval 20–800°C using a vibrating sample magnetometer in a field of intensity of 50 Oe under low vacuum. The powder of investigated alloy was cold-pressed into small tablets having diameter of about 3 mm. The samples were heated up to 800°C with heating and cooling rate kept at 4 K/min.

In order to investigate the changes in structure and phase composition that have direct influence on magnetic properties, caused by TM, corresponding micro-structural analyses and magnetic measurements were carried out before (in optimized magnetic state) and after the TM.

Phase composition and crystallite size of the rapid-quenched Nd-Fe-B alloy were determined by X-Ray powder diffraction (XRD) analysis. For the XRD data collection a Philips_Xcelerator automated X-ray powder diffractometer was used. The diffractometer was equipped with a Co-tube. The generator was set-up on 40 kV and 30 mA. A fixed divergence slit 0.76 mm was used. Data for the Rietveld refinement were collected in a continuous mode between 20 and 110° 2θ. Intensity was averaged at every 0.002° 2θ.

The X-ray line-broadenings were analyzed by Fullprof software [4]. In the Fullprof program, X-ray line broadenings were analyzed through refinement of the

Thompson Cox Hastings-pseudo Voight (TCH-pV) function parameters, in this case most reliable peak-shape function. For the instrumental broadening correction, standard specimen LaB_6 was used. XRPD pattern of the standard was fitted by convolution to the experimental TCH-pV (U= 0.002815; V= -0.003345; W= 0.001761; X= 0.000076; Y= 0.040512 for $CoK\alpha_1$ and U= 0.006021; V= -0.004091; W= 0.001481; X= 0.000076; Y= 0.040512 for $CoK\alpha_2$). Average values of the apparent size and mixing strain are averaged over all directions in the reciprocal space. Values in the parentheses measure degree of anisotropy of the apparent size and maximal strain. Details of the applied models could be found elsewhere [4].

Quantitative phase analysis was done by the FullProf [4] computer program. For quantitative analysis sample was carefully prepared to comply with the definition of a "powder": homogeneity and sufficient number of particles with random orientation. According to Brindley [5] and Hill & Howard [6], in a mixture of N crystalline phases the weight fraction W_j of phase j is given by:

$$W_j = \frac{(S_j Z_j M_j V_j)/\tau_j}{\sum_i (S_i Z_i M_i V_i)/\tau_i} \qquad ....(1)$$

where: S_j is the scale factor of phase j, Z_j is the number of formula units per unit cell for phase j, M_j is the mass of the formula unit, V_j is the unit cell volume, τ_j is the Brindley particle absorption contrast factor for phase j defined as:

$$\tau_j = \frac{1}{V_j} \int \exp\{-(\mu_j - \mu_u)x\}dV_j \qquad ...(2)$$

where: V_j is the volume of a particle of phase j, μ_j is the particle linear absorption coefficient, μ_u is the mean linear absorption coefficient of the solid material of the powder, x is the path of the radiation in the particle of phase j when reflected by the volume element dV_j. The latter parameter accounts for microabsorption effects that become important when the compounds of the powder have rather different linear absorption coefficients. Its calculation requires only the knowledge of the particle radius and linear absorption coefficient μ. We have assumed that particle radius for all phase was 15 μm.

Magnetic properties of alloy i.e. corresponding hysteresis loops were obtained at ambient temperature using Quantum Design MPMS 5XL Superconducting Quantum Interference Device (SQUID) magnetometer with magnetic field strength in range − 50 to 50 kOe.

3. Results and Discussion

The rapid quenched $Nd_{14}Fe_{79}B_7$ alloy in optimized magnetic state was investigated by thermomagnetic measurement. Fig. 1. shows the thermomagnetic curves that bring the information about phase composition modification and magnetic behaviour in temperature interval 20–800°C.

The obtained TM curves Fig. 1., suggest nearly monophase composition of the investigated alloy with dominant presence of hard magnetic $Nd_2Fe_{14}B$ phase and the small amount of soft magnetic α-Fe phase with high saturation magnetization.
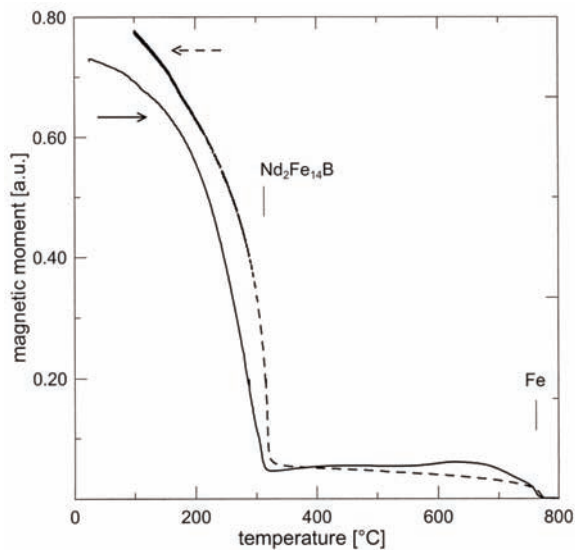
Fig. 1. Thermomagnetic curves of investigated $Nd_{14}Fe_{79}B_7$ alloy

The X - ray diffractograms of $Nd_{14}Fe_{79}B_7$ powder in state before and after thermomagnetic measurement are shown on Fig. 2. By observing the results of XRD analysis for both investigated states, the hard magnetic phase $Nd_2Fe_{14}B$ is identified as the primary phase [7]. The presence of boride phase $Nd_{1.1}Fe_4B_4$ and α–Fe was also found out and some small amount of unidentified components was also detected. Due to low reflections intensity and a great number of reflections of the identified primary phase, it was difficult to strictly define by this analysis to which phases the unidentified diffraction maximums belong. They obviously represent remnant minor paramagnetic phases, predominantly those of high Nd content being situated on grain boundaries [8,9,10]. The Fe-Nd corresponds to ferro-magnetically ordered phases, up to the $Fe_{17}Nd_5$ intermetallics and to the paramegnetically ordered Fe-Nd phases with higher Nd content.

To obtain a better understanding of the influence of phase composition and crystallite size of the identified phases on the magnetic properties before and after TM, size-strain and quantitative phase analyses of the XRD data were performed.

The amount of the hard and soft magnetic phases and their crystallite sizes, calculated by Full-Prof program are presented in Table 1. and Table 2.

Different ability of phases to absorb X-rays was taken into account for the calculation of content of crystalline phases. The results of XRD show very good agreement with the results of chemical analysis. For the sample in the optimized magnetic state (before TM), mass amounts of each cation (per gram of the sample) calculated from the phase mass percentages are: Nd - 25.35 %, Fe - 73.70 %, B - 0.95 %. After the TM individual atom mass contents are: Nd - 28.11 %, Fe - 70.18 %, B - 0.75 %, O - 0.81 %. When judging the validity of the obtained agreement, partial oxidation of the sample after the TM should be considered.

The results of quantitative phase XRD analysis of the Nd-rich $Nd_{14}Fe_{79}B_7$ alloy in the optimized magnetic state (Fig. 2.a, Table 1) suggest that the alloy has almost monophase composition with dominant amount of hard magnetic $Nd_2Fe_{14}B$ phase (95 mass%). The presence of other soft and paramagnetic phases such as α-Fe, $Nd_{1.1}Fe_4B_4$ and phases of Fe-Nd, Fe-B type were determined as well. Nevertheless, due to low intensities of diffraction peaks of these phases, the contents and mean grain sizes were calculated only for $Nd_2Fe_{14}B$ and α-Fe phase.

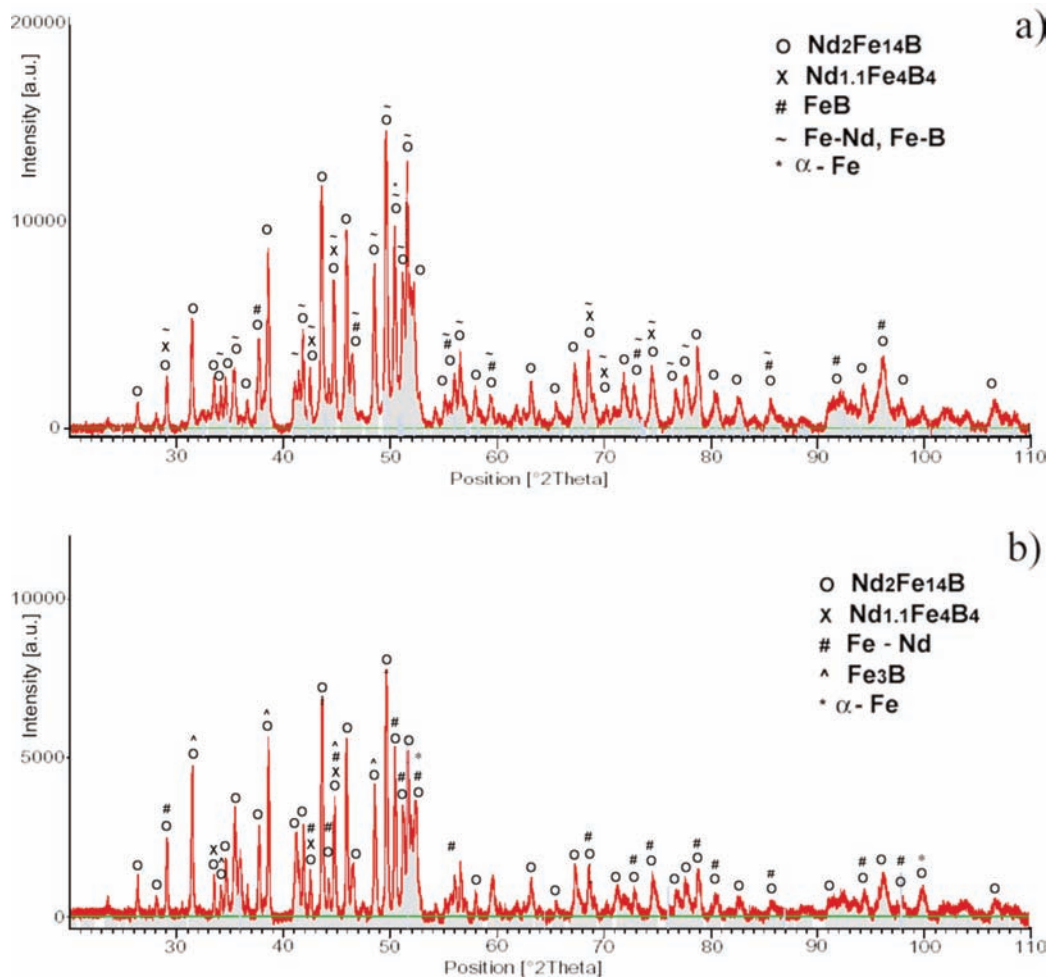The results of quantitative and crystallite size analyses of XRD data (Fig. 2.b and

Fig. 2. The X-ray diffractograms of Nd$_{14}$Fe$_{79}$B$_7$ powder in

a) optimized magnetic state and b) after thermomagnetic measurements

Table 2.) for the alloy in state after TM measurement show evident decrease of the amount of Nd$_2$Fe$_{14}$B phase and the increase of crystal grain size. While the content of main hard magnetic Nd$_2$Fe$_{14}$B phase in optimized state is estimated to 95 mass% in state after TM measurements it is reduced to 75 mass%. The amount of soft magnetic phases after TM has noticeably increased, predominantly of Fe$_{17}$Nd$_5$ phase. The hexagonal Fe$_{17}$Nd$_5$ phase exhibits easy plane anisotropy, and therefore, reduces

value of coercivity [15]. The amount of the Fe$_{17}$Nd$_5$ and Nd$_2$O$_3$ phases in the state after TM measurement is about ~ 20mass% with grain size much smaller than hard magnetic phase. The presence of Nd$_2$O$_3$ phase can be explained by oxidation of Nd-rich phases during the TM measurements. Besides, Al$_{6.3}$B$_{88}$ and Fe$_3$B phases were also identified but taking into account their complex crystal structure they were not considered.

Results of microstructural analysis (Table1., Table2.) show that the majority of

Table 1. Unit cell parameters, Brindley factors, size-strain parameters and R-factors for $Nd_{14}Fe_{79}B_7$ alloy in optimized magnetic state

	$Nd_2Fe_{14}B$		α-Fe	
	refined	literature data [11]	refined	literature data [12]
a [Å]	8.80548(9)	8.803(1)	2.86783(8)	2.8665(2)
b [Å]	8.80548(9)	8.803(1)	2.86783(8)	2.8665(2)
c [Å]	12.22288(1)	12.196(1)	2.86783(8)	2.8665(2)
α [°]	90	90	90	90
β [°]	90	90	90	90
γ [°]	90	90	90	90
V [Å³]	947.719(1)	945.1	23.821(1)	23.55
Bridnley factor τ	0.986	-	1.024	-
Mass percentage [%]	95.0(5)	-	5.00(8)	-
Average appar. size [Å]	571.41(1.15)	-	596.96 (0.18)	-
Average max. strain x10^4	2.72	-	7.79	-
R-factors not corrected for background				
R_{wp}	2.00	-	2.00	-
R_p	1.33	-	1.33	-
χ^2	3.82	-	3.83	-
Conventional Rietveld R-factors				
R_{wp}	16.9	-	25.7	-
R_p	19.6	-	24.4	-
χ^2	3.82	-	3.83	-

phases that are present in the investigated material have high degree of crystallinity i.e. small number of defects in microstructure. Large sizes of crystallites and low values of microstrain support this. Refined parameters of the unit cells of $Nd_2Fe_{14}B$ and α-Fe phases are in good correspondence to the values found in literature. However, refining of the unit cell parameters of $Fe_{17}Nd_5$ and Nd_2O_3 phases was not possible due to high complexity of these systems and very low degree of crystallinity, as confirmed by high values of microstrain.

Generally speaking, in the optimal magnetic state the single grains of the hard magnetic phase that are more or less separated by a paramagnetic RE-rich boundary phase can cause decoupling of magnetic $Nd_2Fe_{14}B$ grains, thus reducing the remanence enhancement by reducing the exchange-coupling effect. On the other side, the isolation of magnetic $Nd_2Fe_{14}B$ grains by non-magnetic phases can lead to the increase of coercivity. The other important parameter is the grain size, since both coercivity and the exchange-coupling effect are the sensitive functions of grain size. An increase in grain size generally results in decrease of coercivity and remanence enhancement [9].

Practically, the increase of the amount of the soft magnetic phases and the increase of the grain size of present phases have the direct influence on reduction of magnetic

Table 2. Unit cell parameters, Brindley factors, size-strain parameters and R-factors for $Nd_{14}Fe_{79}B_7$ alloy after thermo-magnetic measurements

	$Nd_2Fe_{14}B$		α-Fe		$Fe_{17}Nd_5$		Nd_2O_3	
	refined	literature data [11]	refined	literature data [12]	refined	literature data [13]	refined	literature data [14]
a [Å]	8.79436(6)	8.803(1)	2.86783(8)	2.8665(2)	20.214	20.214	3.831	3.831
b [Å]	8.79436(6)	8.803(1)	2.86783(8)	2.8665(2)	20.214	20.214	3.831	3.831
c [Å]	12.2038(1)	12.196(1)	2.86783(8)	2.8665(2)	12.329	12.329	5.999	5.999
α [°]	90	90	90	90	90	90	90	90
β [°]	90	90	90	90	90	90	90	90
γ [°]	90	90	90	90	120	120	120	120
V [Å^3]	943.85(1)	945.1	23.586(1)	23.55	4362.78	4362.78	76.25	76.25
Bridnley factor τ	1.045	-	1.316	-	0.892	-	0.700	-
Mass percentage [%]	75.0(5)	-	3.35(8)	-	13.8(4)	-	5.7(2)	-
Average appar. size [Å]	629	-	340	-	64	-	171	-
Average max. strain x10^4	3.2	-	5.1	-	8.1	-	8.5	-
R-factors not corrected for background								
R_{wp}	3.16	-	3.16	-	3.16	-	3.16	-
R_p	1.83	-	1.83	-	1.83	-	1.83	-
χ^2	6.81	-	6.81	-	6.81	-	6.81	-
Conventional Rietveld R-factors								
R_{wp}	25.7	-	25.7	-	25.7	-	25.7	-
R_p	24.4	-	24.4	-	24.4	-	24.4	-
χ^2	6.81	-	6.81	-	6.81	-	6.81	-

properties.

For investigated $Nd_{14}Fe_{79}B_7$ alloy in optimized magnetic state experimentally obtained value of coercive force and remanence measured on VSM are $_iH_C$ = 16.2 kOe, Br = 7.4 kG. Maximal magnetic energy is 10.6 MGOe, which is expected value for Nd-Fe-B alloy with ~90 mass% of hard magnetic phase [16]. Measured values of magnetic properties suggest that in the state before TM measurement the optimal phase composition and optimal microstructure were obtained. Magnetic behaviour of investigated alloy before and after TM is presented on Fig. 3 with the corresponding SQUID hysteresis loops.

The shape of the SQUID hysteresis loop of the Nd-rich Nd-Fe-B alloy in the optimized magnetic state (Fig. 3.) implies the presence of the magnetically decoupled nanocrystalline structure and shows high hard magnetic quality of the alloy, as none of the material contains any significant content of "parasitical" phases which could derogate hard magnetic properties. The obtained high
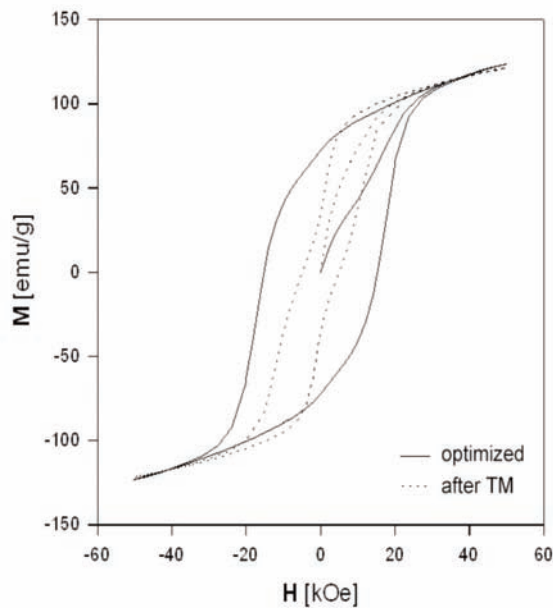
Fig. 3. SQUID hysteresis loops of $Nd_{14}Fe_{79}B_7$ alloy in optimized magnetic state and after the thermomagnetic measurement

value of coercivity ($_jH_c$ = 16.2 kOe) supports this and indicates nearly a monophase structure of the alloy with dominant content of main hard magnetic phase $Nd_2Fe_{14}B$ (95 mass%).

The saturation magnetization of $Nd_{14}Fe_{79}B_7$ alloy in optimized magnetic state at the maximum magnetic field strength of 50 kOe was 123 emu/g (12.5 kG). However, the expected saturation magnetization of the alloy containing 90 mass% of $Nd_2Fe_{14}B$ phase is 15.6 kG, [16]. It can be that the measured values were below the expected value, probably because the maximum magnetic field of 50 kOe is not high enough to cause magnetic saturation of the main hard magnetic $Nd_2Fe_{14}B$ phase [17].

The influence of phase transformations which have occurred during TM measurement and the growth of crystal grains (Table 1., Table 2.) on the magnetic properties of the investigated alloy is clearly illustrated with a quality loss of the hard magnetic properties that can be observed on SQUID hysteresis loop (Fig. 3.) for the state after TM.

4. Conclusions

Changes in the structure parameters, phase composition and crystallite size of rapid quenched Nd-rich $Nd_{14}Fe_{79}B_7$ alloy, caused by thermomagnetic measurements have been studied using XRD methods of phase analysis, crystallite size and lattice microstrain determination.

Obtained results of XRD and microstrain analyses of the investigated alloy in the optimized magnetic state suggest that the alloy has nearly monophase composition with dominant amount of hard magnetic $Nd_2Fe_{14}B$ phase (up to 95 mass%) with mean crystallite size below 60 nm. The presence of small amount (up to 5 mass%) of -Fe and other Nd-rich phases is determined as well. However, these nanocrystalline phases situated on grain boundaries of $Nd_2Fe_{14}B$ phase have probably influenced formation of magnetically decoupled nanocrystalline structure of the investigated alloy.

From the magnetic point of view, changes of phase composition during the TM, first of all, decrease of the amount of hard magnetic $Nd_2Fe_{14}B$ phase (up to 75 mass%), increase of the amount of soft magnetic and oxide phases as well growth of crystallites of present phases had direct influence on degradation of the hard magnetic properties of this alloy observed in the state after TM.

The shape of the obtained SQUID hysteresis loop indicates high coercive magnetically decupled nanocrystalline structure of the alloy in optimized magnetic state as well, witch is characteristic for Nd-rich Nd-Fe-B alloys. On the other side, the SQUID hysteresis loop for the alloy in the state after TM, clearly illustrates derogation of hard magnetic properties, as a consequence of structural and phase transformations.

Acknowledgement

References

1. O. Gutfleisch, J. Phys. D: Appl. Phys., 33 (2000) 157.

2. N. Talijan, V. Ćosović, J. Stajić-Trošić, T. Žák, J. Magn. Magn. Mat., 272–276 (2004) e1911.

3. A. Grujić, N. Talijan, A. Maričić, J. Stajić-Trošić, V. Ćosović, V. Radojević, Sci. Sint., 37 (2005) 139.

4. Rodriguez-Carvajal J FullProf.2k (Version 2.40-May 2003-LLB JRC) Computer program; www-llb.cea.fr/fullweb/fp2k/fp2k.htm

5. G. W. Brindley, Phil. Mag. 36 (1945) 347.

6. R. J. Hill, C. J. Howard, J. Appl. Cryst. 20 (1987) 467.

7. J. Stajić-Trošić, PhD Thesis, University Of Belgrade, 2005.

8. D. Goll, H. Kronmüller, Naturwissenschaften, 87 (2000) 423.

9. Yu. D. Yagodkin, A. S. Lileev, J. V. Lyubina, et al., J. Magn. Magn. Mater., 258-259 (2003) 586.

10. V. Ćosović, N. Talijan, A. Grujić, J. Stajić-Trošić, T. Žák, Z. Lee, V. Radmilović, Sci. Sint., 41 (2009) 209.

11. J. F. Herbst, J. J. Croat, W.B. Yelon, J. Appl. Phys. 57 (1984) 4086.

12. E. A. Owen, E. L. Yates, J. Chem. Phys. 3 (1935) 605.

13. J. Moreau, L. Paccard, J. P. Nozieres, F. P. Missell, G. Schneider, V. Villas-Boas, J. Less-Common Met., 163 (1990) 245.

14. J. X. Boucherle, J. Schweizer, Acta Crystallogr., Sect. B: Struct. Sci, 31 (1975) 2745.

15. F. J. G. Landgraf, F. P. Missell, H. R. Rechenberg, G. Schneider, V. Villas-Boas, J.M. Moreau et al., J Appl Phys 70 (1991) 6125.

16. J. Ding, Y. Lee, P.T. Yong, J. Phys. D: Appl. Phys., 31 (1998) 2745.

17. E. F. Kneller, R. Hawig: Ieee Trans. Magn., 27 (1991) 3589.